Universidade de Aveiro Departamento de Biologia
Ano 2017

CAROLINA SOFIA PEREIRA ROXO

AVALIAÇÃO DO POTENCIAL CITOTÓXICO DE NANOMATERIAIS DE GRAFENO

EVALUATION OF THE CYTOTOXIC POTENTIAL OF GRAPHENE NANOMATERIALS

DECLARAÇÃO

Declaro que este relatório é integralmente da minha autoria, estando devidamente referenciadas as fontes e obras consultadas, bem como identificadas de modo claro as citações dessas obras. Não contém, por isso, qualquer tipo de plágio quer de textos publicados, qualquer que seja o meio dessa publicação, incluindo meios eletrónicos, quer de trabalhos académicos.

Universidade de Aveiro Departamento de Biologia
Ano 2017

CAROLINA SOFIA PEREIRA ROXO

AVALIAÇÃO DO POTENCIAL CITOTÓXICO DE NANOMATERIAIS DE GRAFENO

EVALUATION OF THE CYTOTOXIC POTENTIAL OF GRAPHENE NANOMATERIALS

Tese apresentada à Universidade de Aveiro para cumprimento dos requisitos necessários à obtenção do grau de Mestre em Biologia Molecular e Celular, ramo da Biologia, realizada sob a orientação científica da Doutora Helena Cristina Correia de Oliveira, Investigadora de Pós-doutoramento do Departamento de Biologia do Centro de Estudos do Ambiente e do Mar – CESAM e do Instituto de Materiais de Aveiro-CICECO da Universidade de Aveiro e sob co-orientação do Prof Doutor Fernando José Mendes Gonçalves, Professor Associado e com Agregação do Departamento de Biologia e do Centro de Estudos do Ambiente e do Mar – CESAM da Universidade de Aveiro.

Apoio financeiro da Fundação para a Ciência e Tecnologia pelo projeto ERASIINN/0003/2013

Dedico este trabalho à minha mãe e irmão, pelo enorme apoio dado na realização deste objetivo de vida.

o júri

presidente

Prof. Doutora Maria Paula Polónia Gonçalves
Professora associada da Universidade de Aveiro

Arguente principal

Doutor José Miguel Pimenta Ferreira de Oliveira
Professor Auxiliar Convidado, Departamento de Biologia – Faculdade de Ciências – Universidade do Porto

Orientadora

Doutora Helena Cristina Correia de Oliveira
Investigadora Pós-Doutoramento, CESAM - Centro de Estudos do Ambiente e do Mar do Instituto de Materiais de Aveiro-CICECO da Universidade de Aveiro

agradecimentos

Primeiramente quero agradecer à minha mãe e irmão por todo o apoio e compreensão dados nestes últimos dois anos. Agradeço à Universidade de Aveiro por me terem acolhido como aluna do Mestrado de Biologia Molecular e Celular, à Dra Helena Oliveira por me ter aceite no seu projeto e por ser minha mentora, que me ensinou, apoiou e incentivou a trabalhar mais e melhor e ao Prof. Dr. Fernando Gonçalves por me ter recebido no seu grupo para poder realizar o projeto de tese de mestrado. Agradeço também aos meus colegas de trabalho em laboratório que me apoiaram e me ajudaram sempre que precisei, Bruna Teixeira, Fábio Campos e Catarina Menezes.

palavras-chave

GFN's, Citotoxicidade, Raw 264.7, Internalização, ROS, Apoptose, Potencial de Membrana Mitocondrial, Citometria de Fluxo

resumo

O grafeno tem a espessura de um único átomo de carbono, de duas dimensões, arranjado de forma hexagonal e desde o seu isolamento, as suas propriedades têm sido bastante estudadas, sendo o grafeno e os materiais baseados no grafeno aplicados em diversas áreas. Vários tipos de nanomateriais de grafeno têm sido sintetizados e vastamente aplicados, contudo existe ainda algum desconhecimento acerca dos seus potenciais efeitos na saúde humana, sobretudo porque estes nanomateriais podem ser facilmente inalados, especialmente no processo de manufatura, caso não existam os devidos cuidados.

Neste trabalho, um conjunto de compostos de grafeno foram selecionados para avaliação do seu efeito citotóxico em macrófagos RAW264.7. Como referência foi usado o bem caracterizado negro de carvão. As células foram expostas às doses BMD30 e 0.5BMD30, definidas por estudos anteriores. Para tal avaliou-se o grau de internalização das diferentes GFNs (família dos nanomateriais de grafeno) pelas células RAW264.7, assim como os potenciais efeitos oxidativos pela avaliação na produção de ROS. Os GFNs P4, P5 e P6 foram selecionados para estudos adicionais devido ao seu alto potencial tóxico. Foram estudados os mecanismos de morte induzida para os GFNs P4, P5 e P6 pela avaliação da percentagem de células em apoptose / necrose e pelo potencial de membrana mitocondrial.

Os resultados mostraram que todos os GFNs testados foram internalizados pelas células RAW 264.7, mas a P3, P4 e P5 (carboxil grafeno, nanoplaquetas de grafeno e óxido de grafeno de camada única, respetivamente) foram internalizados em proporções mais altas. Para P1, P2, P3, P5 e P6, observou-se um aumento na internalização de nanomateriais dependente da duração de exposição aos mesmos. Além disso, os GFNs P2, P3, P4, P6 e P8 mostraram um aumento da produção de ROS nas concentrações de 0.5BMD30, mas não nas concentrações de BMD30. Os resultados mostraram que P4 e P5 aumentaram o número de células apoptóticas e a diminuíram o potencial da membrana mitocondrial nas células RAW 264.7.

Em geral, os nossos resultados demonstraram que a toxicidade dos GFNs é amplamente dependente das suas características físico-químicas, sugerindo que de todos os GFNs estudados, os P4 e P5 (nanoplaquetas de grafeno e pó de óxido de grafeno de camada única, respetivamente) foram os mais citotóxicas para as células RAW264.7.

keywords

GFN´s, Cytotoxicity, Raw264.7, Uptake, ROS, Apoptosis, Mitochondrial Membrane Potential, Flow Cytometry

abstract

Graphene is a single-atom thick, two-dimensional sheet of hexagonally arranged carbon atoms and since its isolation, its properties have been widely studied, and graphene and graphene-based nanomaterials are now applied in several fields. Several types of graphene-family nanomaterials (GFN) have been synthesized and widely applied, but there is still some misunderstanding about their potential effects on human health, especially since these nanomaterials can be easily inhaled, especially in the manufacturing process, if they are not properly cared for.

In this work, a set of graphene family compounds were selected for the evaluation of their cytotoxic effects on RAW264.7 macrophages. The well-characterized Carbon black nanomaterial was used as reference. Cells were exposed to the BMD30 and 0.5 BMD30 doses defined in previous studies. The internalization of the different GFNs (graphene-family nanomaterials) compounds by RAW264.7 cells was evaluated, as well as its potential oxidative effects by the evaluation of the production of reactive oxygen species (ROS). The GFNs P4, P5 and P6 were selected for further studies due to their highest toxicity potential. The mechanisms of GFNs induced cell death were studied for P4, P5 and P6 by the evaluation of the percentage of cells under apoptosis/necrosis and the mitochondrial membrane potential.

The results showed that all the GFNs tested were internalized by RAW 264.7 cells, but P3, P4 and P5 (carboxyl graphene, graphene nanoplatelets and single layer graphene oxide, respectively) were internalized at higher ratios. For P1, P2, P3, P5 and P6 an increase in nanomaterial internalization with exposure duration was observed. Furthermore, the GFNs P2, P3, P4, P6, and P8 showed an increase of ROS production at 0.5BMD30 but not at BMD30 concentrations. The results showed that P4 and P5 increased the number of apoptotic cells and decreased mitochondrial membrane potential of RAW 264.7 cells.

Overall our results demonstrate that the toxicity of GFNs is widely dependent on their physico-chemical characteristics, suggesting that from all the GFNs studied, P4 and P5 (graphene nanoplatelets and single layer graphene oxide powder, respectively) were the most cytotoxic to RAW264.7 cells.

List of Tables and Figures

List of Acronyms and Abbreviations

- 1D: One-Dimensional
- 2D: Two-Dimensional
- 3D: Three-Dimensional
- ATP: Adenosine Triphosphate
- BMD: Bench Mark Dose
- BSA: Bovine Serum Albumin
- BALF: Broncho Alveolar Lavage Fluid
- CNT: Carbon Nanotubes
- CVD: Chemical Vapor Deposition
- DCF: 2',7'-Dichlorfluorescein
- DCFH: 2',7'-Dichlorofluorescin
- DCFH2-DA: Dichloro-Dihydro-Fluorescein Diacetate
- DMEM: Dulbecco's Modified Eagle's Medium
- FBS: Fetal Bovine Serum
- FCM: Flow Cytometry
- FITC: Fluorescein Isothiocyanate
- FS: Forward Scatter
- GFNs: Graphene-Family Nanomaterials
- GO: Graphene Oxide
- MMP: Mitochondrial Membrane Potential
- MWCNT: Multi-Walled Carbon Nanotubes
- rGO: Reduced Graphene Oxide
- ROS: Reactive Oxygen Species
- SS: Side Scatter
- SD: Standard Deviation
- SWCNT: Single-Walled Carbon Nanotubes
- PBS: Phosphate-Buffered Saline
- PCD: Programmed Cell Death
- PI: Propidium Iodide
- PS: Phosphatidylserine

Table of Contents

I. Introduction

Nano Etymology and Classification

Nanomaterials, considered the building blocks for nanotechnology, are engineered materials with one or more components with at least one dimension measuring 100 nm or less. The current definition of nanomaterial is the one adopted by the European Union in 2011, in which a nanomaterial is “a natural, incidental or manufactured material containing particles, in an unbound state or as an aggregate or as an agglomerate and where, for 50 % or more of the particles in the number size distribution, one or more external dimensions is in the size range 1 nm - 100 nm” (Fig.1). In addition, “By derogation from the above, fullerenes, graphene flakes and single wall carbon nanotubes with one or more external dimensions below 1 nm should be considered as nanomaterials” (European Commission 2011).

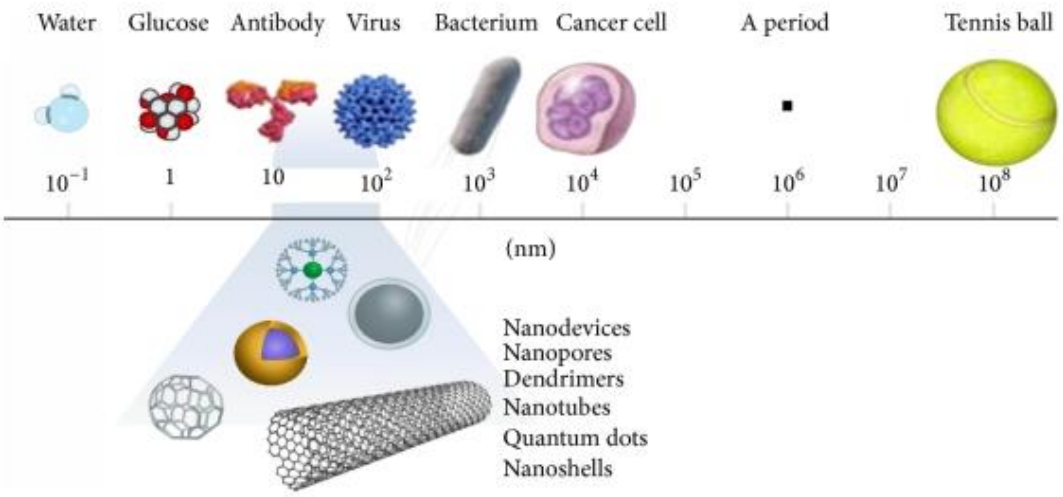

Figure 1: A size comparison of nanoparticle with other larger-sized materials. Adapted from Amin et al., 2014

Nanoparticles can be then classified according to their size and also according to their dimensions (1D, 2D, 3D); their morphology, as for instance flatness, sphericity and aspect ratio; their composition, if they are composed of single material or several materials; their uniformity and agglomeration (Buzea et al.,

2007). Therefore, in the category of nanomaterial are included the nanoparticles, nanofibers and nanotubes, composite materials and nano-structured surfaces (Bussy et al., 2012). The International Organization for Standardization defined the term nano-object as a material with one, two or three external dimensions in the nanoscale, shown in Fig. 2. Nanoparticles can have different shapes or crystalline form, and their surfaces can act as transporters for liquid droplets or gases. In a certain way nanoparticulate matter should be considered a distinct state of matter, in addition to the solid, liquid, gaseous, and plasma states, due to its distinct properties (Buzea et al., 2007).

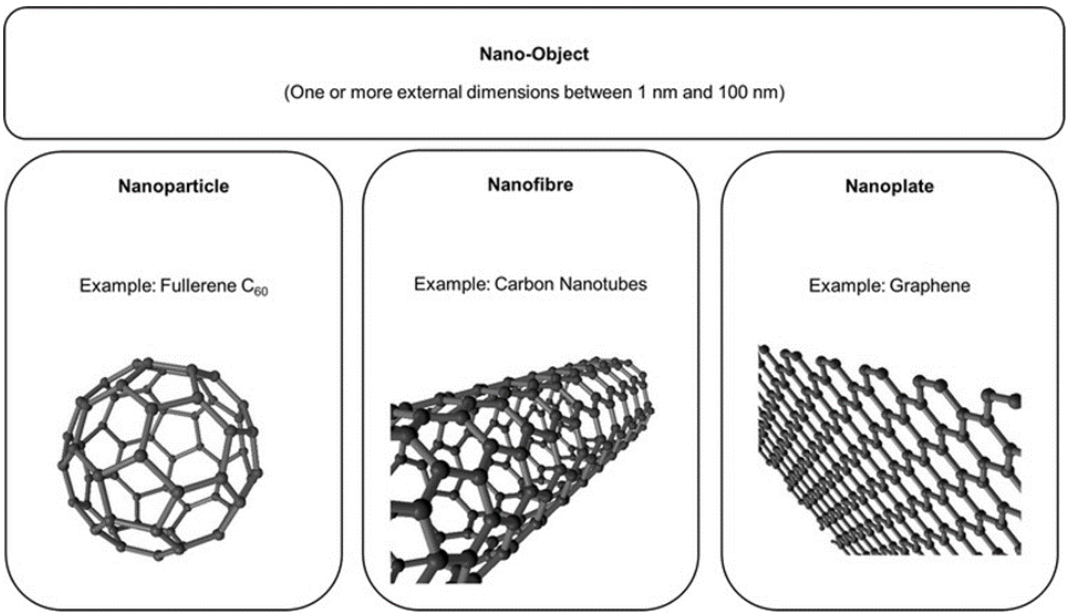

Figure 2: The different Nano-Objects. Adapted from Omlor et al.,2015

Nanotechnology

The concept of nanotechnology was introduced by the Nobel Prize laureate Richard Feynman, in 1959 in his lecture in the meeting of the American Physical Society “There’s plenty room at the bottom” (Feynman, 1960). However, the term Nanotechnology was first coined only several years later by the Japanese researcher Norio Taniguchi, in 1974 (Stern and McNeil, 2008).

Nanotechnology can be defined as the design, synthesis, and application of materials and devices whose size and shape have been engineered at the

nanoscale. It exploits unique chemical, physical, electrical, and mechanical properties that emerge when matter is structured at the nanoscale (Buzea et al., 2007). Nanotechnology is a promising molecular technology present in several areas of science and has many technological applications (Suzuki et al., 2007). With this, nanomaterials have increased their importance in the field of consumer products and nanodevices because of their unique structural, optical, physiochemical, magnetic, and surface characteristics (Suzuki et al., 2007; Kumar et al., 2011).

Carbon-based Nanomaterials – Graphene Nanomaterials

Carbon-based nanomaterials are a superfamily that includes fullerenes, carbon nanotubes (CNT), diamond, graphite and graphene, all of them allotropes of carbon (Hirsch 2010; Ma-Hock et al., 2013). In terms of scope of applications CNTs and graphene seem to be the more developed. Despite their common carbon-based elemental consistency, CNTs and graphene are two very distinct nanomaterial entities (Bussy et al., 2012). CNTs can be single-walled (SWCNT) or multi-walled (MWCNT) carbon sheets (Fig. 3) (Ma-Hock et al., 2013). Graphene is a more recent discovery, first isolated by Novoselov and Geim (Geim, 2009) and consists of a a single-atom thick, two dimensional sheet of hexagonally arranged carbon atoms isolated from graphite, and is a strong and light material that conducts heat and electricity extremely well (Sanchez et al., 2012; Park et al., 2014). Since graphene was isolated, its properties have been widely studied, and graphene and graphene-based nanomaterials are now applied in several fields, including electronics, energy storage, biosensors and biomedicine (Park et al., 2015).

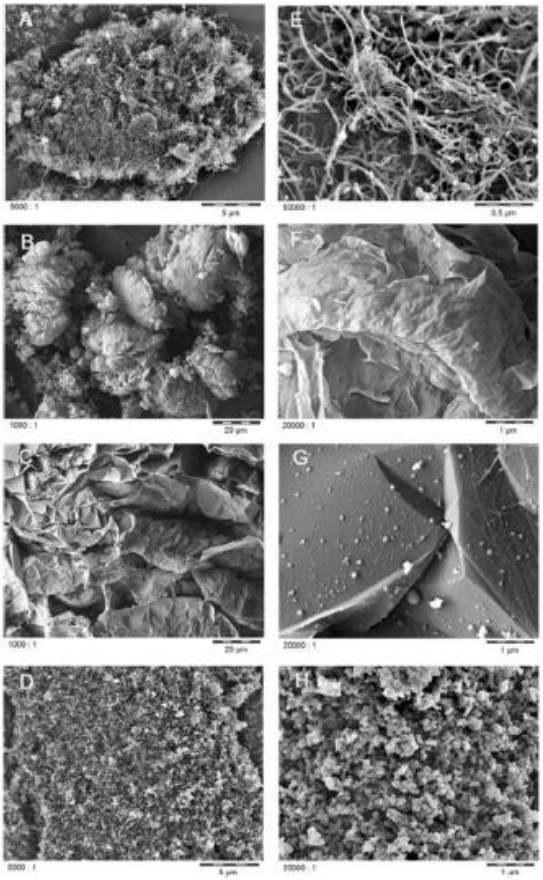

Figure 3: **Scanning electron microscopy images of the test materials**. A-D: agglomerate scale, E-H: primary structure scale. A, E: MWCNT, B, F: graphene, C, G: graphite nanoplatelets, D, H: Carbon Black. Note the same scale for MWCNT and Carbon Black, and slightly different set of scales for graphite nanoplatelets and graphene, in order to point to their individual characteristics. Adapted from Ma-Hock et al., 2013

Graphene is one of the members of a much broader family of graphene-based materials, the Graphene-Family Nanomaterials (GFNs), and it includes few-layer graphene (FLG), graphene nanosheets (GNS), graphene oxide (GO) and reduced graphene oxide (rGO). They vary in layer number, lateral dimension, surface chemistry, defect density or quality of the individual graphene sheets, and composition and purity (Sanchez et al., 2012).

GFNs have different preparation methods that can be classified into two categories: top-down organic synthetic approaches and bottom-up organic synthetic approaches. Top-down approaches, such as mechanical cleavage, the redox method, and arc discharge, utilize natural graphite as the carbon source and yield single- or few-layered graphene and GO through physical or chemical exfoliation or shear. Bottom-up approaches, such as CVD (Chemical vapor

deposition) and organic synthesis, utilize small carbon compounds to synthesize large single- or few-layered graphene and GO (Zhang et al., 2017).

Graphene Applications

Graphene has highly attractive properties such as high specific surface area, excellent electronic conductivity, thermal conductivity and mechanical strength, with this, graphene and its derivatives have revealed potential in several fields. In electronics, for example, it has been used for broadband and ultrafast photo-detection and optical modulation. It is used for water filtration and desalination, in energy technology, sensors and catalysis, but biomedical application is a relative new area with substantial potential. The use of graphene in biomedicine has many applications, such as drug/gene delivery, biological sensing, and imaging, antibacterial materials, to biocompatible scaffold for cell culture and cancer treatments as detector of cancer biomarkers (Sanchez et al., 2012; Shen et al., 2012; Sing, 2016;).

Nanotoxicology and Graphene Toxicity

Nanotoxicology was suggested as a new branch of toxicology to report the adverse health effects caused by nanoparticles (Buzea et al., 2007). Humans can be exposed to nanoparticles by several exposure routes, as for instance inhalation, ingestion, dermal penetration, injection or implantation for biomedical applications. Due to their small size, nanoparticles can translocate from these entry portals into the circulatory and lymphatic systems, and ultimately to tissues and organs. Some nanoparticles, depending on their composition and size, can produce irreversible damage to cells by oxidative stress and/or organelle injury. (Buzea et al., 2007; Sanchez et al., 2012). In a context of environment contamination or work place exposure, inhalation is a major route of exposure. The risk of exposure by inhalation is increased when GFNs are synthesized as dry powders using thermal exfoliation.

Experimental studies in rodents demonstrated that instillation of SWCNT and MWCNT can cause pulmonary inflammation, granulomas, fibrosis, and ultimate

death. Therefore, the extensive use of graphene nanoparticles and their derivatives bring concerns regarding their safety (Stern and McNeil, 2008) and potential impact on the human health and the environment (Bussy et al., 2012; Ou et al., 2017).

Inhalation is thought to be an important route of nanoparticle exposure because of their aerodynamic sizes that can lead to inhalation, traveling great distances in air, and substantial deposition in the human respiratory tract. This may impair lung defence and clearance leading to formation of granulomas and lung fibrosis (Suzuki et al., 2007; Stern and McNeil, 2008). Clearance mechanisms in the lung include the mucocilliary escalator and phagocytosis by alveolar macrophages, and some studies in rodents demonstrated that nanoparticles deposited in the lungs can translocate to the pulmonary interstitium (Stern and McNeil, 2008). Long-term and chronic exposure to GFNs may result in some diseases or harm health condition, for instance causing Parkinson's disease- like symptoms by inducing cell apoptosis and senescence (Ou et al., 2017).

The toxicity of GFNs depends of the dose, shape, surface chemistry, exposure route, and purity, and these properties play an important role in the toxicity of GFNs (Sing, 2016). GO demonstrated to induce cytotoxicity in several cell types, generation of ROS and decrease viability of cells (Wang et al., 2013), This effect was observed, for instance on HLF cells and A549 cells (Chang et al., 2011; Wang et al., 2013). Furthermore, in the kidney HEK293T cells GO caused DNA damage and loss of cell viability (Lu et al., 2017). GO nanosheets, in RAW264.7 cells, induced cell-cycle alterations, apoptosis and ROS (Matesanz et al., 2012).

GO and rGO in HepG2 cells induced NADPH oxidase, ROS formation, apoptosis – related genes expression and caused plasma membrane damage (Chatterjee et al., 2014).

Pristine graphene in RAW264.7 cells can induce cytotoxicity through the depletion of the mitochondrial membrane potential (MMP), increase intracellular reactive oxygen species (ROS), then trigger apoptosis by activation of the mitochondrial pathway (Li et al., 2012; Rastogi et al., 2017), also in RAW264.7, resulted in elevated transcription and secretion of cytokines and chemokines and further alter the morphology and function of naïve macrophages (Zhou et al., 2012).

Graphene nanoplatelets (GNPs) down-regulated the generation of ROS, suppressed ATP production and caused mitochondria damage in BEAS-2B (Park et al., 2015).

The still limited literature on *in vitro* toxicity propose that GFNs can be also benign or toxic to cells, and the biological reaction will differ through the material family depending on layer number, lateral size, stiffness, hydrophobicity, surface functionalization, and dose (Sanchez et al., 2012; Singh et al., 2011).

Numerous groups have reported extremely low cytotoxicity and excellent biocompatibility of GO sheets. In contrast, some other groups have detected the cytotoxicity of graphene based materials due to the generation of harmful ROS, cell membrane damage by the sharp edge of graphene sheets, or wrapping the cells by aggregating graphene sheets in a suspension (Zhou et al., 2014). Particle numbers and surface area are important in the dose–response assessment of nanotoxicity. Size, shape, aggregation, surface functionalization/charge and the protein binding of the carbon nanomaterials may change the diffusion and sedimentation of these materials in cell culture systems, which directly influence the cellular dose of these materials, this can explain the controversial results in toxicity of graphene (Zhang et al., 2014; Zhou et al., 2014).

II. Assay techniques and biomarkers to assess nanoparticle toxicity

Uptake Potential of GFN´s

The uptake of nanoparticles by cells is an important factor to assess nanotoxicity. Nanoparticles internalization by the cells can be identified by flow cytometry (FCM) by assessing the changes in light scattering or fluorescence. When particles are taken up by the cells the side-scatter (SS) intensity increases without change the forward-scatter (FS), as shown in Figure 4. This evaluation of uptake potential of nanoparticles using SS e FS is proper for initial screening of nanotoxicity (Ibuki and Toyooka, 2012).

Recent observations in biological systems suggest that the physical parameters of nanoparticles can affect their nonspecific uptake in cells, with potential to induce cellular responses (Jiang et al., 2008).

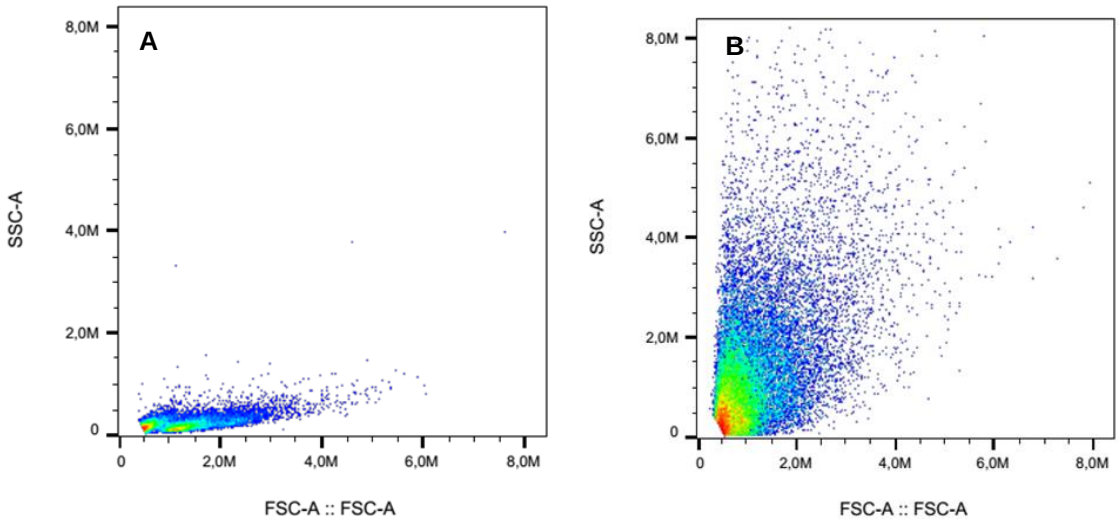

Figure 4: Changes on flow cytometry light scattering upon exposure to nanoparticles. A- Control cells; B- Cells exposed to P4

Cellular Uptake Mechanism

Endocytosis is a common entry mechanism of several extracellular materials and the process is energy dependent, which means it will be hindered when incubations are carried out in an adenosine triphosphate (ATP)-depleted environment. The endocytosis pathway includes phagocytosis for larger foreign materials and pinocytosis for soluble materials or nanoparticles. Pinocytosis can be divided into four subcategories (Fig.5): macropinocytosis, for particles with a diameter between 0.5-5µm; clathrin-dependent endocytosis, for particles with a diameter between 200-500nm, and clathrin- and caveolae-independent endocytosis, for particles between 100-150nm (Huang et al., 2012).

Macrophages are the ultimate cells of differentiation of the mononuclear phagocyte system, forming an important component of immunity doing phagocytosis of foreign bodies as well as in warning the rest of the immune system against invaders to cause innate or adaptive immune response. They are implicated in tissue repair and wound heling activities, being also a shield against

invading pathogens, toxicants or particles like graphene nanoparticles. If graphene nanoparticles originate toxicity to macrophages, there will be substantial damage in the immune resistance capacity of subjects (Arora et al., 2017; Sasidharan et al., 2012).

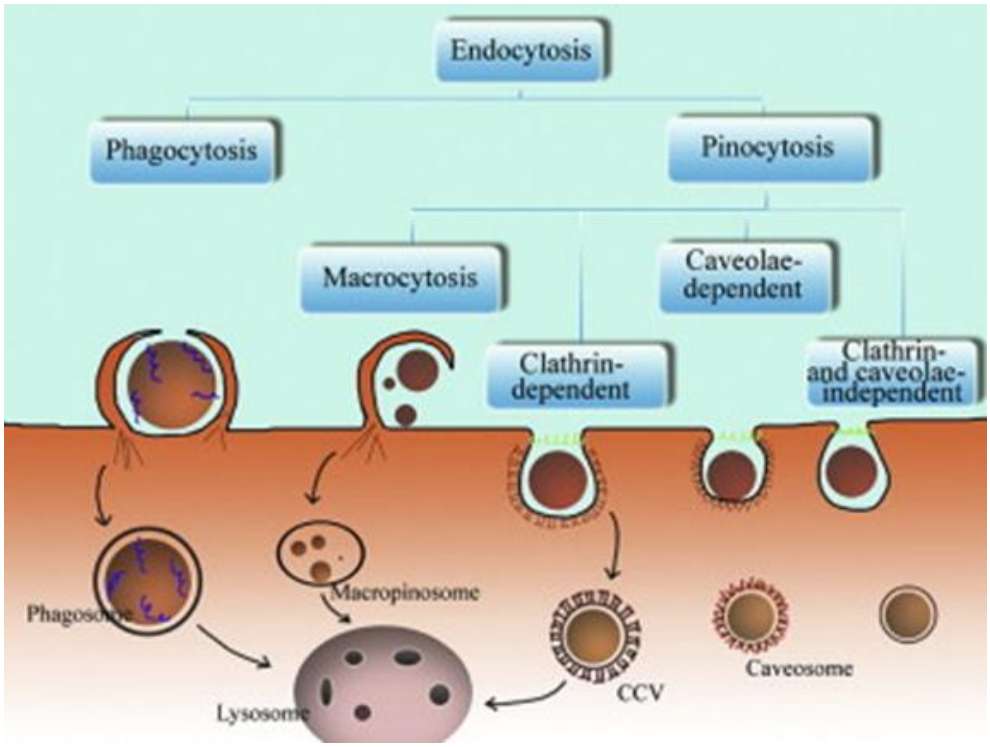

Figure 5: Cellular Uptake Mechanism. Adapted from Kou et al., 2013

Bussy, and co-workers (2012) summarised the main uptake mechanisms of GFNs following their interaction with membranes: phagocytosis, membrane adsorption and receptor-mediated endocytosis.

Reactive Oxygen Species

Reactive oxygen species (ROS) are important to intermediate in oxidative metabolism. However, when generated in excess, ROS can damage cells by peroxidising lipids and damaging structural proteins, enzymes and nucleic acids, resulting in necrosis, apoptosis or malignancy (Sing, 2016; Zhang et al., 2014). To evaluate the intracellular oxidative stress, the cell permeable oxidation-sensitive probe DCFH-DA may be used to determine the generation of ROS in the presence

of GFNs. DCFH-DA is a non-fluorescent molecule that can be easily transported across the cell membrane and deacetylate by esterase's to form non-fluorescent 2',7'-dichloorfluorescin (DCFH), which becomes trapped inside the cells and gets further converted to highly fluorescent 2',7'-dichloorfluorescein (DCF) in the presence of peroxidases (Zhou et al., 2014).

As with other nanomaterials, a presumptive source of GFN cytotoxicity in eukaryotic cells is direct or indirect generation of intracellular ROS. An indirect source of intracellular ROS can result from impurities produced during GFN synthesis or chemical modifications of graphene. Direct sources of intracellular ROS include edge defects of graphene sheets or internal defects to GO sheets (for example) produced during synthesis. Both indirect and direct sources for GFN-generated ROS have the potential to interfere with biochemical processes and induce cytotoxicity and genotoxicity (Zhang et al., 2014).

Cellular Apoptosis

Apoptosis or programmed cell death (PCD) defines a genetically-encoded cell death program, which is morphologically, biochemically and molecularly distinct from necrosis. Necrosis is only the passive result of cellular injury and apoptosis forms an integral part of normal physiological cell processes. Apoptosis ensures a balance between cell proliferation and cell death and plays a regulatory role in the control of the size of cell populations and tissues (Vermes et al., 2000).

The apoptotic process is characterized by specific morphologic features, including loss of plasma membrane asymmetry and attachment, plasma membrane blebbing, condensation of the cytoplasm and nucleus, and internucleosomal cleavage of DNA (Hingorani et al., 2011; Ly et al., 2003; Vermes et al., 2000). Loss of plasma membrane asymmetry is one of the earliest features of apoptosis. In apoptotic cells, the membrane phospholipid phosphatidylserine (PS) is translocated from the internal to the outer leaflet of the plasma membrane, thereby exposing PS to the external cellular environment. Annexin V is a Ca^{2+} -dependent phospholipid-binding protein with high affinity for PS, and binds to exposed apoptotic cell surface PS. Annexin V can be conjugated to fluorochromes while retaining its high affinity for PS and thus serves as a sensitive probe for FCM

analysis of cells undergoing apoptosis. PS translocation leads to the loss of membrane integrity, which accompanies the later stages of cell death resulting from either apoptotic or death. Therefore, staining with Annexin V is typically used in conjunction with propidium iodide (PI) for identification of early and late apoptotic cells. Viable cells with intact membranes exclude PI, while the membranes of dead and damaged cells are permeable to PI. Consequently, cells that are considered viable are both Annexin V and PI negative, while cells that are in early apoptosis are Annexin V positive and PI negative, and cells that are in late apoptosis are Annexin V and PI positive and dead cells are Annexin V negative and PI positive (Fig.6) (Hingorani et al., 2011).

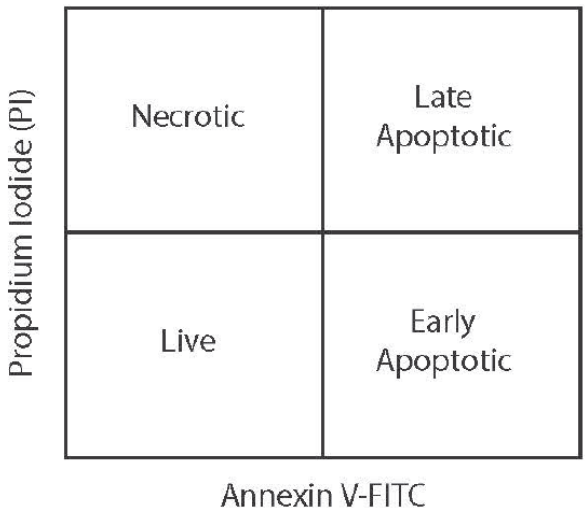

Figure 6: Identification of apoptotic cells by FCM

Mitochondrial Membrane Potential

Mitochondrial membrane potential (MMP) has an important role in intermediate the oxidative energy metabolism, specifically maintaining the physiological function of the respiratory chain to generate ATP, and is capable of producing energy that supports aerobic conditions (Gerencser et al., 2012; Gottlieb et al., 2013; Joshi and Bakowska, 2011).

Several ways to indicate molecular probes and methods have been used to evaluate the electrical potential through the mitochondrial membrane, like the

probe Rhodamine 123 (Joshi and Bakowska, 2011; Scaduto et al., 1999) distributes passively between the cytosol and mitochondria, where transmembrane dissemination depends of the membrane potential, so it will respond to both changes in mitochondrial potential and in plasma membrane potential. In case of collapse of MMP, a reduction in fluorescence intensity occurs (Ly et al., 2003).

III. Cell Line RAW264.7

The cell line RAW 264.7 is a macrophage cell line, isolated from *Mus musculus* (mouse) and this line was established from a tumour induced by Abelson murine leukaemia virus (Fig. 7).

This cell line is easy to propagate, highly efficient for DNA transfection, sensitivite to RNA interference, and supports replication of murine noroviruses.

The base medium for this cell line is ATCC-formulated Dulbecco's Modified Eagle's Medium (DMEM) whit 10% of glutamine, fungizone, pen-strep and fetal bovine serum (FBS) and their culture conditions are with the atmosphere at 95% of air, and 5% of carbon dioxide (CO2) and the temperature at 37°C. Regarding to the culture properties, RAW264.7 is adherent cells that grow in a nonolayer. (ATCC, 2016).

Figure 7: RAW 264.7 Cells

IV. Aims

The general aim was to perform a comprehensive study on the cytotoxicity of seven graphene nanomaterials to macrophage RAW 264.7 cells using carbon black as reference, to establish a toxicity ranking.

The specific aims of this work were:

- To evaluate the internalization of the several GFNs at 0.5 BMD30 and BMD30 and to evaluate the influence of structure on the uptake potential by flow cytometry;
- To study the potential of the several GFNs to induce ROS production in RAW 264.7 cells;
- To evaluate the effect of GFNs on the induction and modulation of early and late apoptosis/necrosis;
- To study the effects of GFNs on the mitochondrial membrane potential
- To establish a cytotoxicity ranking of the several GFNs.

V. Materials and Methods

Test Materials and Characterization

For the current study 7 GFNs compounds were selected (P1-P7) and carbon black (P8) was used as reference for particulate material (Table 1):

P1. Single-Layer Graphene Powder;
P2. Single-Layer graphene from factory series;
P3. Carboxyl graphene;
P4. Graphene nanoplatelets;
P5. Graphene oxide powder (S method);
P6. Graphite oxide powder;
P7. Reference pristine graphene nanoplatelets;
P8. Reference Carbon Black particles

Table 1: Shows the detailed information of the several nanomaterials

Sample	Source Product	Diameter (μm)	Thickness	Specific surface (m^2/g)	SEM image	Preparations/ Properties
P1	ACS GN1P 0005	~5	2-10	278 (400-1000)	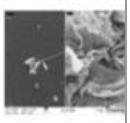	Thermal exfoliation reduction + Hydrogen reduction
P2	ACS GN1PF	0.5-5	2-10	620 (650-750)	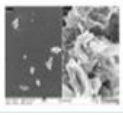	1-5 atomic layer graphene nanosheets
P3	ACS GN1PF 010	1-5	0.8-1.2	1.5	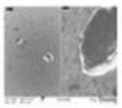	1 – Modified Hummer's method to make graphene oxide; 2 – Convert –OH and C-O-C into –COOH. Carboxyl ratio: 5%
P4	ACS GNNP 0051	~5	2-10	15 (20-40)	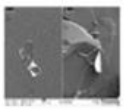	Stacks of multi-layer graphene, with a high aspect ratio, width to thickness
P5	ACS GNOS 0010	1-15	0.8-1.2	5.2 (5-10)	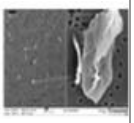	Stauden-maier method; oxygen content: 35%
P6	ACS GTOP 0002	0.5-5	1-3	2.7	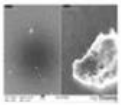	Modified Hummer's method: oxygen content: 35%
P7	AVANZARE	2	3	195 (70)	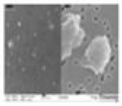	No XPS (low defects by RAMAN) a CS1 carbons. 8±0.5 atomic layer graphene
P8	Evonik-Degussa	14	-	317 (337)	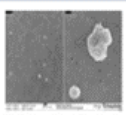	Specified as >99% pure carbon black

Cell Culture

The RAW 264.7 cell line was kindly provided by Dr. Philipp Seib, University of Strathclyde (Glasgow, UK). Cell culture reagents were purchased from Life Technologies (Carlsbad, CA, USA). Cells were grown in Dulbecco's modified Eagle's medium (DMEM), supplemented with 10% fetal bovine serum (FBS), 2 mM L-glutamine, 100 µ/mL penicillin, 100 µg/mL streptomycin, and 250 µg/mL fungizone, at 37 °C in 5% CO_2 humidified atmosphere.

Cells were regularly seen under an Eclipse TS100 inverted microscope (Nikon, Tokyo, Japan) to evaluate their morphology, confluence and screen for possible contaminations. The sub culturing process was done once the cells reached about 70-80% of confluence of the flask surface available for cell growth. Then the old medium was removed, and the cells were washed with phosphate buffered saline – PBS (Gibco). Cells were detached from the flask surface by scraping and then the cells were resuspended in culture medium and counted using a Neubauer Chamber. The desired number of cells were seeded into a new flask and then incubated at the culture conditions described above. The sub culturing process was performed two to three times per week. Standard aseptic techniques were followed throughout the experiments.

GFNs exposure

Cells were seeded in 12 and 6 well plates and incubated for 24h at 37°C, 5%CO_2, for adherence. After the incubation period, the medium was removed and replaced for the same amount of the appropriate dilutions of GFNs. The concentrations for exposure were defined based in previous studies in whichRAW 264.7 cells were exposed to a range of 0.00-50.00 µg/cm^2 GFNs for 24h and 48h and cell viability was assessed by AlamarBlue (AB) and lactate dehydrogenase (LDH) assays (Menezes et al, 2017). The benchmark dose 30 (BMD30) and 0.5 BMD30 of each GFN for 24h were selected for the cell exposure in the subsequent assays and are shown in detail in table 2 (Menezes et al., 2017).

Table 2: Concentrations of particles per area

Particle	Concentration for BMD30 (µg/cm^2)	Concentration for 0.5BMD30 (µg/cm^2)
P1	46.8	23.4
P2	50	25
P3	22	11
P4	25.3	12.65
P5	29.4	14.7
P6	23.6	11.8
P7	50	25
P8	50	25

Uptake Potential of GFNs

Cells were seeded in 6-well plates at 112x10^5 cells/mL for the analysis at 4h and 1x10^5 cells/ml for the analyses at 24h then they were allowed to adhere for 24h. Then, the cells were exposed to each of the GNFs (P1-P7) and carbon black (P8) dispersed in culture medium at the concentrations of BMD30 and 0.5BMD30 respectively and were incubated for 4h at 4ºC (for internalization inhibition) 4h at 37ºC and 24h at 37ºC.

After the incubation period, the cells were scraped, resuspended and collected. The uptake potential was assessed by flow cytometry (FCM) as previously described by (Suzuki et al., 2007). The flow cytometric forward scatter (FS), which gives information on the particles size, and the flow cytometric side scatter (SS) information on complexity of particles, were measured using the Attune® Acoustic Focusing Cytometer (Applied Biosystems). At least 20 000 cells were analysed for each test. The data were analysed by FlowJo software (FlowJo LLC, Ashland, OR, USA).

Reactive Oxygen Species (ROS)

Cells were seeded in 12 wells plates at $1x10^5$ cells/mL and allowed to adhere for 24h. Then the cells were exposed to each of the GFNs P1-P7 and carbon black (P8) dispersed in complete culture medium at the concentrations of BMD30, 0.5BMD30 and incubated for 24h at 37ºC. The control cells were incubated in complete culture medium.

The intracellular levels of ROS were assessed by the oxidation-sensitive probe DCFH-DA. ROS detection was assessed as previously described by Zhou, et al., (2014). After the 24h exposure period, cells were incubated at 37 ºC for 30 min in the dark with fresh medium containing 10 µM DCFH-DA. Thereafter cells were washed with PBS, scraped from the plate wells and resuspended in DMEM medium with 2% of FBS and then collected for analysis by FCM with an Attune® Acoustic Focusing Cytometer (Applied Biosystems) equipped with a 488nm laser. At least 30 000 events were analysed for each test. The data were analysed by FlowJo software (FlowJo LLC, Ashland, OR, USA).

Detection of Apoptosis (Annexin V-FITC/PI Assay)

Cells were seeded in 12-well plates at $1x10^5$ cells/mL and allowed to adhere for 24h. Then, the cells were exposed to the GFNs (P4, P5 and-P6) dispersed in complete culture medium at the concentrations of BMD30, 0.5BMD30 and incubated for 24h at 37ºC. The control cells were incubated in complete culture medium.

Annexin V–fluorescein isothiocyanate (FITC)/propidium iodide (PI) dual staining (BD Biosciences, CA, USA) was employed to detect early/late apoptotic and necrotic cells, and assessed according to manufacturer. After incubation with various GFNs for 24 h, the cells were counted, washed two times with cold PBS and stained with Annexin V and PI. Typically, $1x10^5$ cells were resuspended in binding buffer (100 µL) followed by the sequential addition of FITC-conjugated Annexin V (5µ L; Annexin V–FITC) and PI (5µL). After incubation for 15 min in the dark at room temperature, stained cells were resuspended in binding buffer (400 µL) and directly analysed by FCM with an Attune® Acoustic Focusing Cytometer

(Applied Biosystems). At least 10 000 events were analysed for each test. The data were analysed by FlowJo software (FlowJo LLC, Ashland, OR, USA).

Mitochondrial Membrane Potential (MMP)

Cells were seeded in 12-well plates at $1x10^5$ cells/mL and allowed to adhere for 24h. Then, the cells were exposed to the GFNs (P4, P5 and P6) dispersed in complete culture medium at the concentrations of BMD30, 0.5BMD30 and incubated for 24h at 37ºC. The control cells were incubated in complete culture medium. After de incubation period, cells were washed with PBS and incubated with 5µg/ml^{-1} Rhodamine123 (Sigma-Aldrich) for 30 min, at 37ºC. The cells were washed with PBS, scraped and centrifuged at 800g for 5min, at 4ºC. The cell pellet was washed with 1ml PBS containing 1%BSA (Bovine Serum Albumin) and resuspended in 500µl of PBS containing 1%BSA and 5µg/ml^{-1} PI (Sigma-Aldrich). The cells were analysed by FCM with an Attune® Acoustic Focusing Cytometer (Applied Biosystems) at an excitation wavelength of 488 nm. At least 50 000 events were analysed for each test. The data were analysed by FlowJo software (FlowJo LLC, Ashland, OR, USA).

Statistical analysis

The results are reported as mean ± standard deviation (SD) and for all experiments, at least 3 replicates, and 3 independent assays were performed. Data analysis were performed with the software SigmaPlot version 12.5 (Systat Software Inc.) and the statistical significance between control and exposed cells was performed by one-way ANOVA followed by the Dunn's test as non-parametric test, and Holm-Sidak test for statistically significant difference in the parameters. A *t*-test was used to compare the effect of incubation temperature and duration on GFNs cellular uptake. Normality was tested by the Shapiro-Wilk test. The differences were considered statistically significant for $p < 0.005$.

VI. Results

Cell Characterization

Microscopic observations of cell cultures showed that GFNs exposure decreased cell confluence and increased the number of dead cells (Fig. 8).

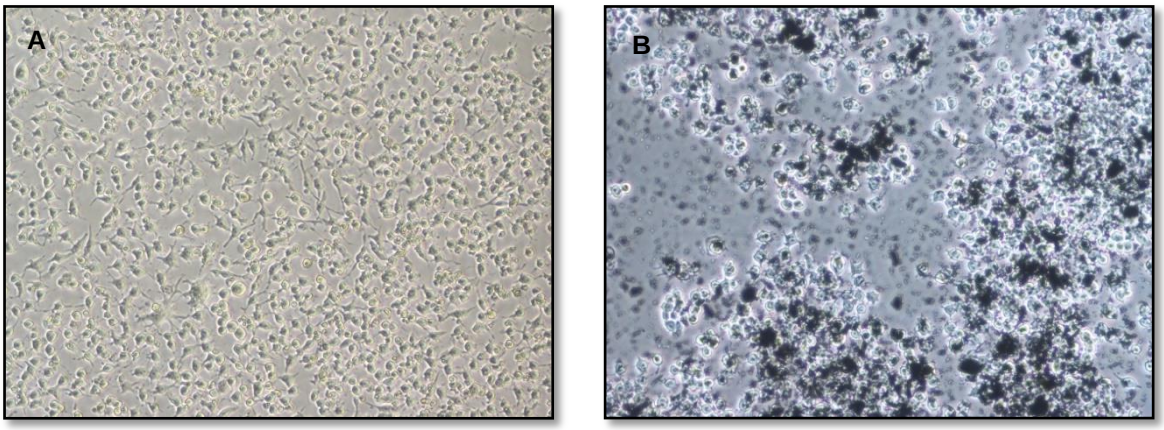

Figure 8: Microscopic images of RAW264.7. A – RAW264.7 cells in control conditions, B - RAW264.7 cells exposed for 24h to 0.5BMD30 of P4.

Uptake Potential of GFNs

The uptake potential of GFNs at 0.5BMD30 and BMD30 in RAW264.7 cells was determined by quantitative analysis of the intracellular SS and measured under three conditions: after a 4h incubation at 4ºC; after a 4h incubation at 37ºC; after a 24h incubation at 37ºC.

Figure 9 shows a representative example of SS vs FS plot of control sample and exposed to P4. Figure 10 shows that overall all the nanomaterials were internalized by RAW264.7 cells. For P1, P2, P3, P5, P6 and P7 both 0.5BMD30 and BMD30 induced an increase in SS. For P4 an increase in SS was also verified but only for the BMD30. The increase in SS upon incubation at 4ºC may indicate adsorption of the nanomaterials to the cell surface. By comparing the internalization after 4h incubation at 4ºC to 37ºC an increase in SS is detected for all the nanomaterials tested at both concentrations in the case of P1, P2, P3, P5 and P6. The effect of duration of the exposure on the levels of internalization was also tested. Results showed that for P2, P3, P4 and P5 the internalization increased with time for both 0.5BMD30 and BMD30 exposures. In the case of P1

this increase occurred only for 0.5 BMD30 and for P6 and P7 it occurred only for BMD30 (Fig. 11).

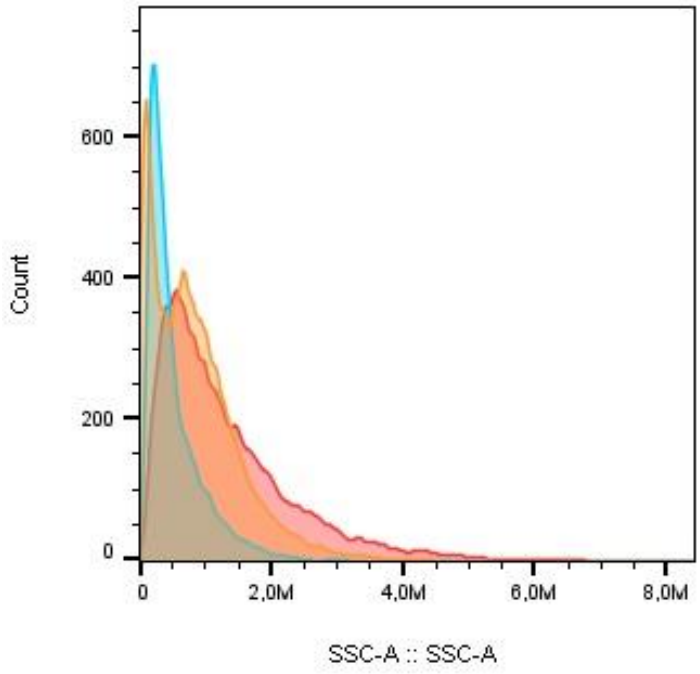

Figure 9 : Uptake potential of P5 by RAW264.7 cells assessed by the side scattered light by flow cytometry. Orange - 4h at 37ºC; Blue - 4h at 4ºC; Red - 24h at 37ºC

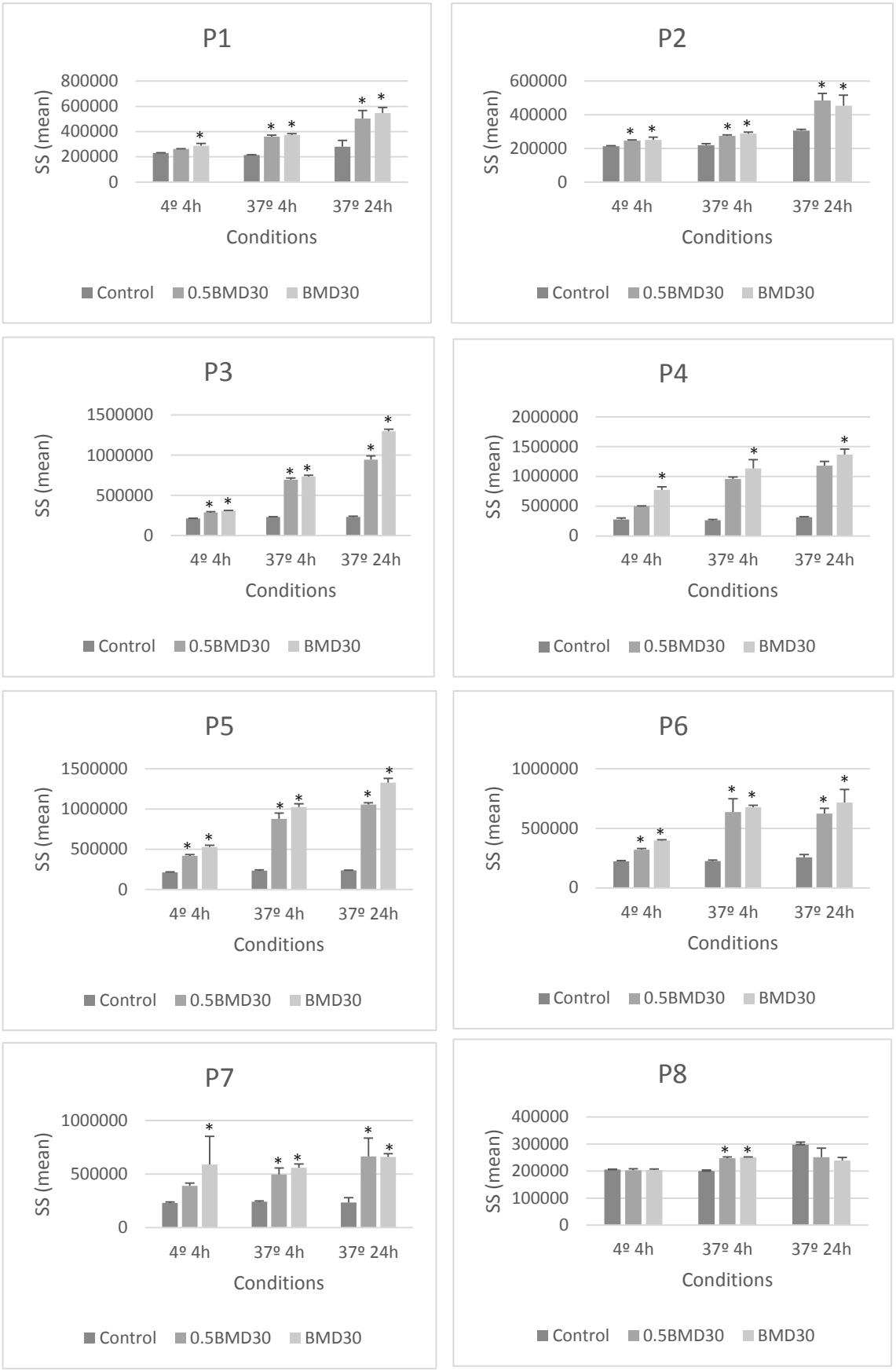

Figure 10: Uptake of GFNs in Raw 264.7 cells. (*) shows the statistically significance difference found upon exposure to GFN's ($P<0.005$). Data shows means ±SD.

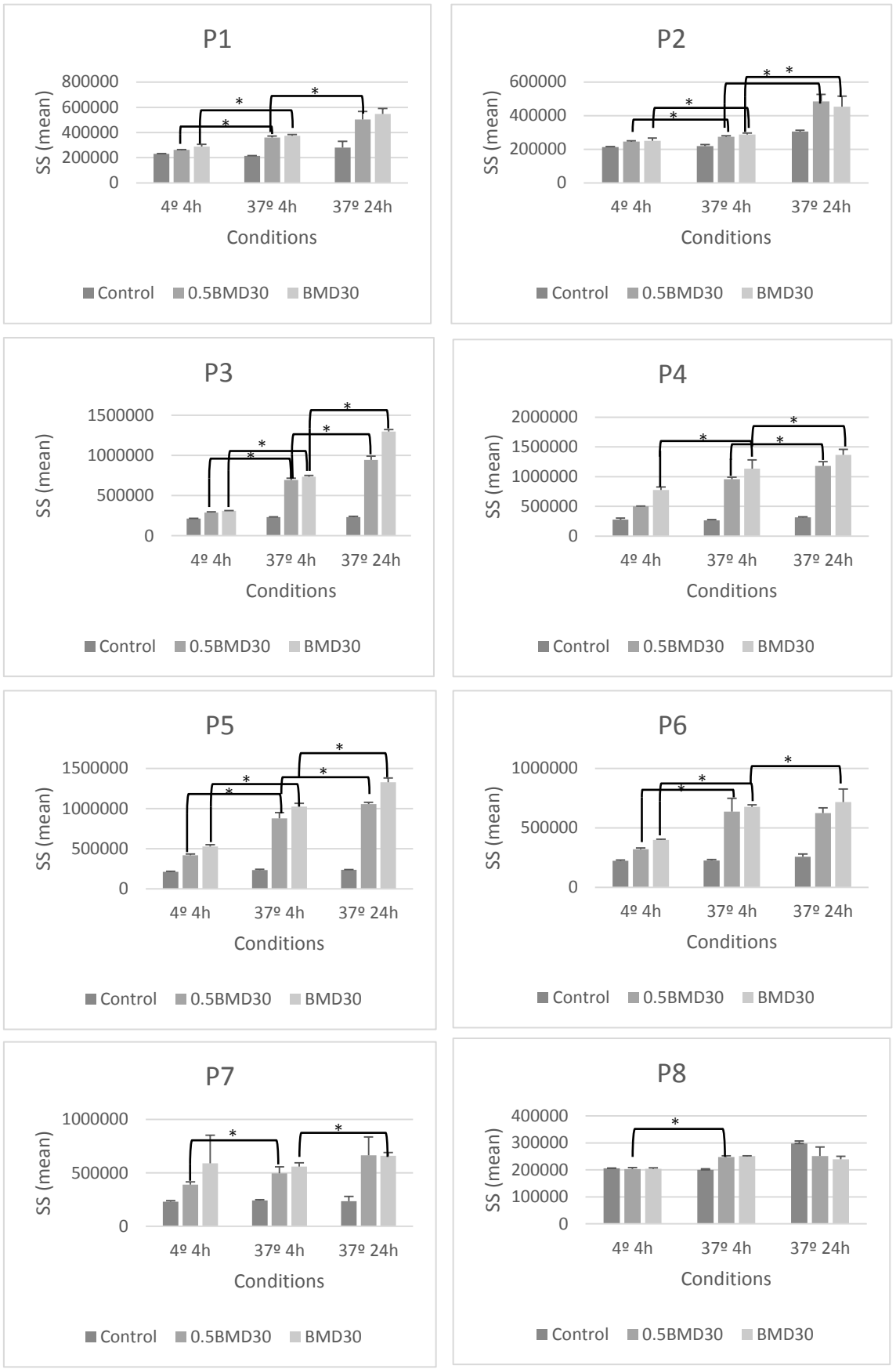

Figure 11: Uptake of GFNs in Raw 264.7 cells, Comparing the time and duration of exposure. (*) shows the statistically significance difference found upon exposure to GFNs (P<0.005). Data shows means ±SD.

Reactive Oxygen Species

The quantification of intracellular ROS in RAW264.7 cells exposed to GFNs for 24h is shown in Figures 12 and 13. The GFNs P2, P3, P4 and P6 and carbon black (P8) at 0.5BMD30 concentration induced an increased in ROS production.

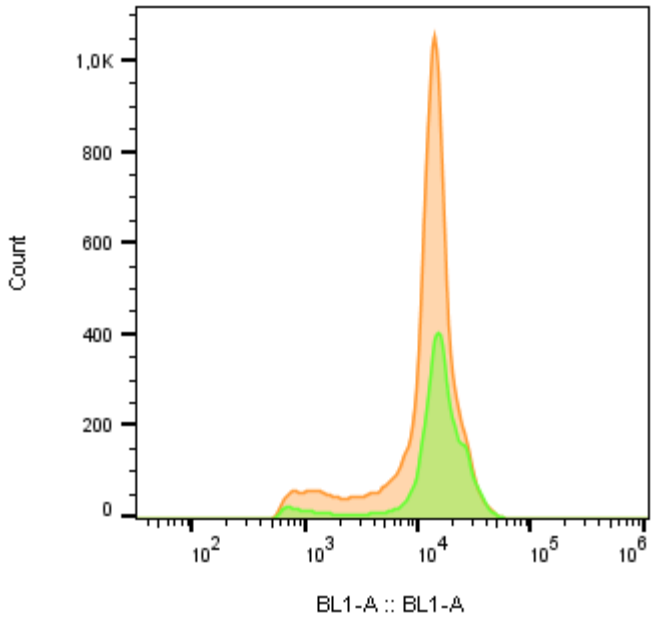

Figure 12: ROS production detected by DCF fluorescence measured by FCM: Orange- Control cells, Green- Cells exposed to P4

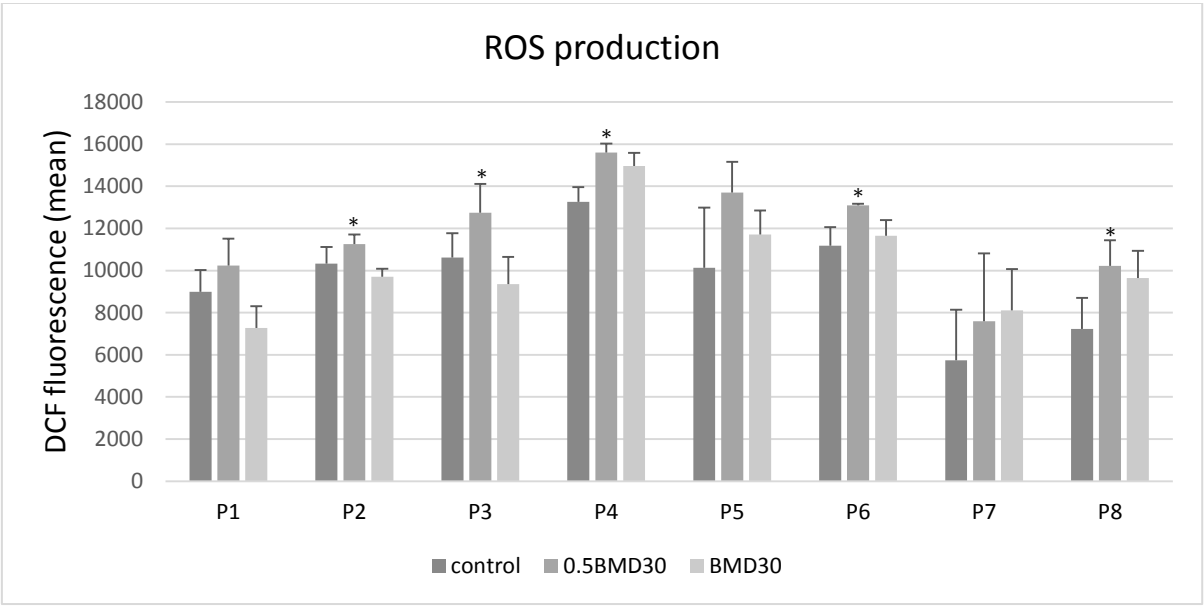

Figure 13: Level of intracellular ROS upon exposure to GFNs. Raw264.7 cells were exposed to GFN's and measured by FCM. (*) shows the statistically significant difference (P<0.005). Data shows means ±SD

Ranking of toxicity

Figure 14 shows the toxicity rankings established based on BMD30 doses for each GFN and the levels of cellular uptake and the ROS production.

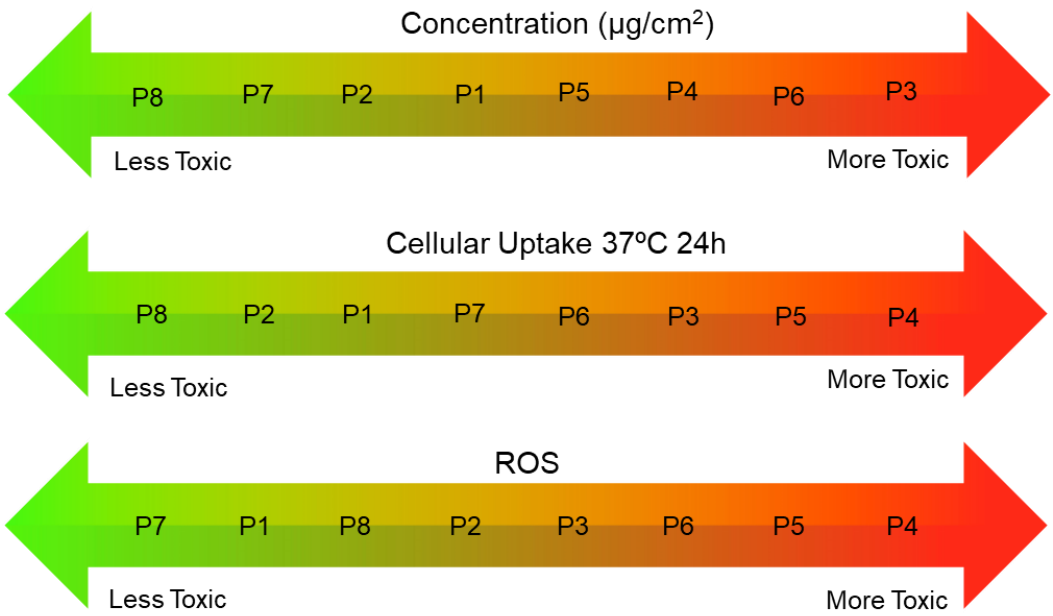

Figure 14: Ranking of toxicity, comparing concentration, cellular uptake and ROS

Cellular Apoptosis

The Annexin V assay was performed in order to evaluate the potential of GFNs to induce apoptosis in RAW264.7 cells. The GFNs P4 (Graphene nanoplatelets (2-10nm thickness)), P5 (Graphene oxide powder (S method)) and P6 (Graphite oxide powder) were selected for this study. As shown in Figures 15 and 16, graphene nano-platelets (P4) induced at 0.5 BMD30 and BMD30 an increase in the percentage of late apoptotic/necrotic cells (A+,P+), and in early apoptotic cells (A+, P-). The percentage of live cells also decreased in both concentrations.

Exposure to graphene oxide (P5) at both 0.5BMD30 and BMD30 also induced an increase in the percentage of late apoptotic/necrotic cells and a decrease in the percentage of live cells (Fig. 17). Exposure to graphite oxide (P6) did not induce any significant changes in the levels of apoptotic cells or live cells (Fig.18).

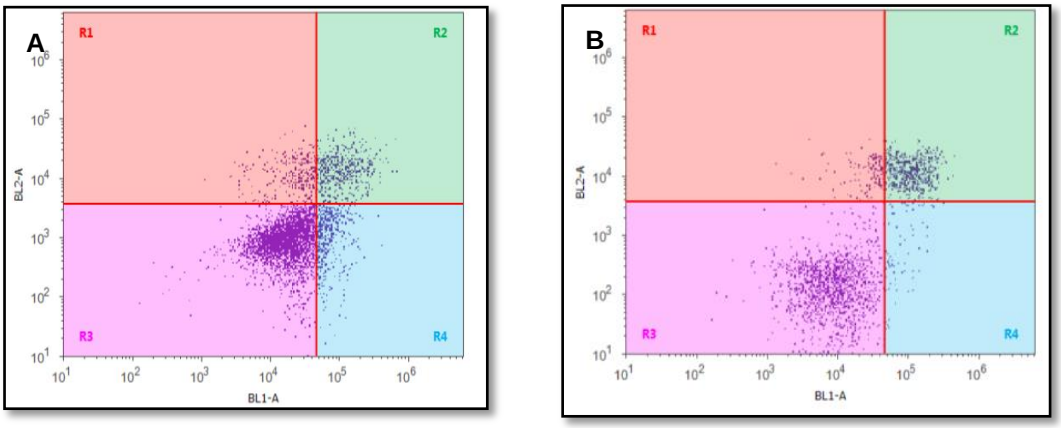

Figure 15: Cellular Apoptosis detected by Annexin-V fluorescence measured by FCM: A- Control cells, B- Cells Exposed to P4

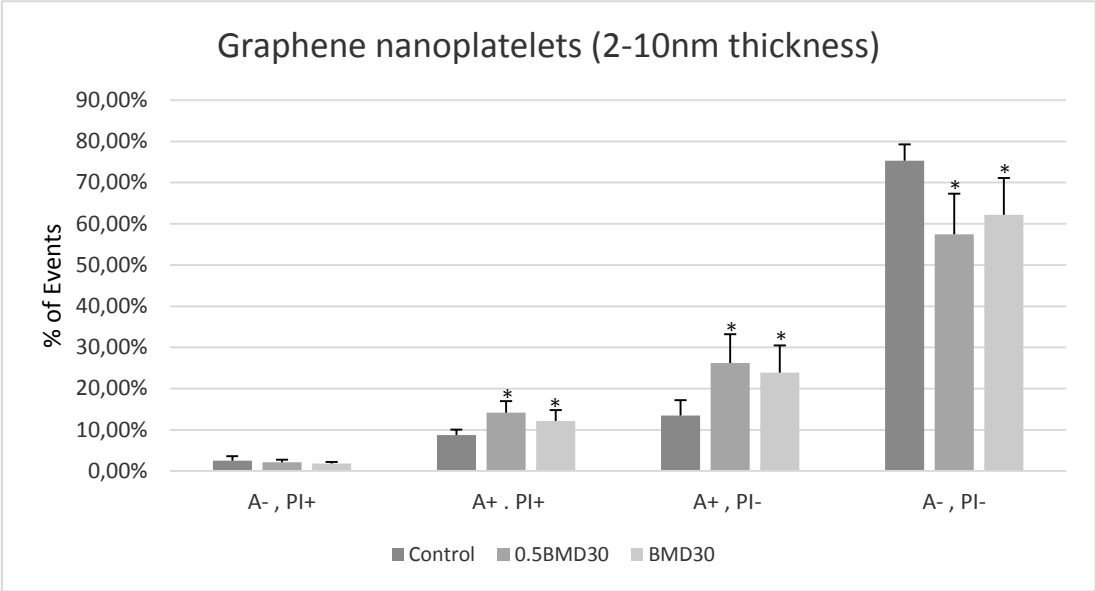

Figure16: Annexin V-FITC and PI assay for apoptosis assessment of Raw264.7 after 24h exposure to particle 4 and measured by FCM. (*) shows the statistically significant difference ($P<0.005$). Data shows means ±SD

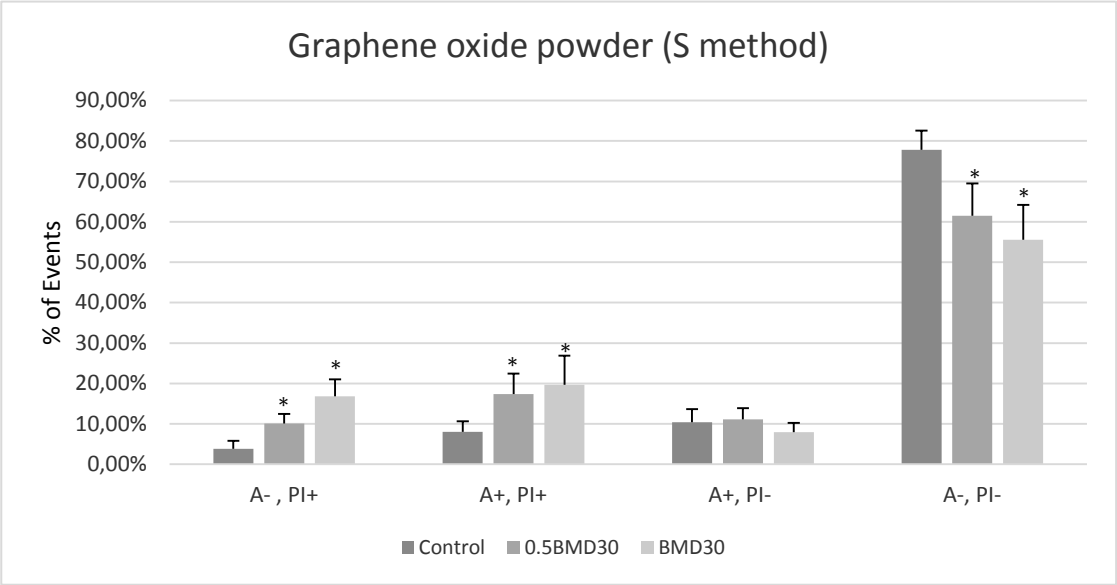

Figure17: Annexin V-FITC and PI assay for apoptosis assessment of Raw264.7 after 24h exposure to particle 5 and measured by FCM. (*) shows the statistically significant difference (P<0.005). Data shows means ±SD

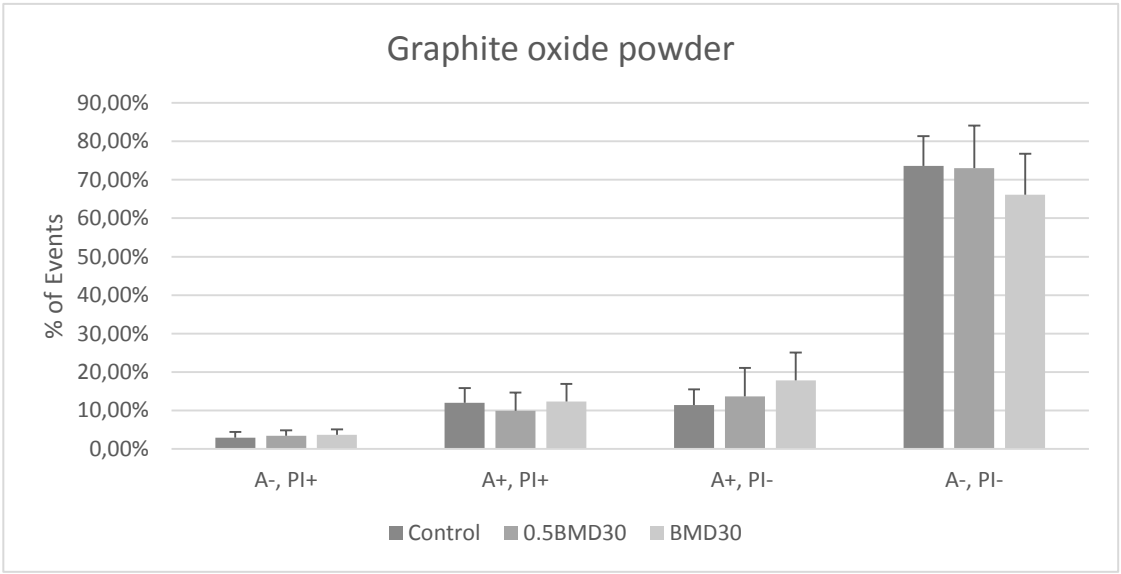

Figure18: Annexin V-FITC and PI assay for apoptosis assessment of Raw264.7 after 24h exposure to particle 6 and measured by FCM. (*) shows the statistically significant difference (P<0.005). Data shows means ±SD

Mitochondrial Membrane Potential

The MMP was measured using the Rhodamine 123 assay by FCM, after RAW264.7 cells exposure to P4, P5 and P6 GFNs for 24h, as show in Figures 19

and 20. Graphene nanoplatelets (P4) at both concentrations induced a decrease in MMP comparatively to the control. For graphene oxide (P5) it was observed a decrease in MMP but only for the highest concentration (BMD30). No changes in MMP were detected upon exposure to P6 at tested concentrations for 24h (Fig. 20).

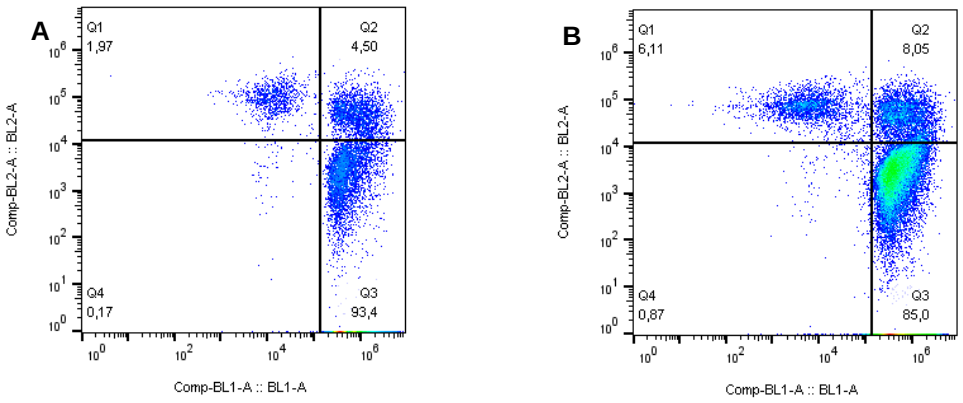

Figure 19: MMP detected by Rhodamine 123 fluorescence measured by FCM: A- Control cells, B – Cells exposed to P4

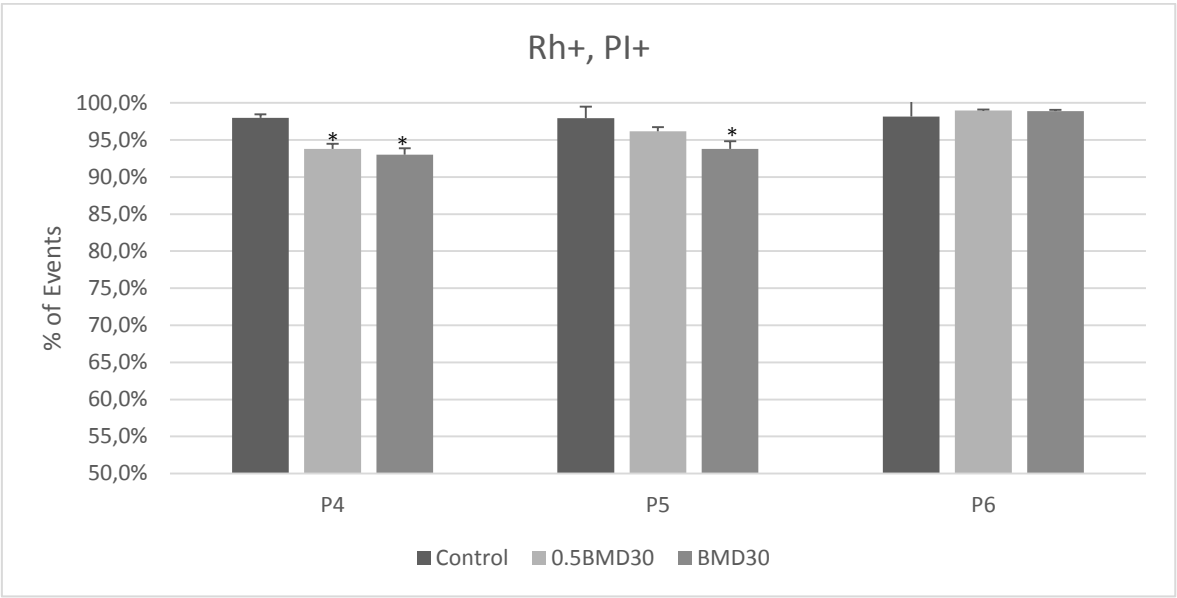

Figure 20: Mitochondrial membrane potential assessment of Raw 264.7 after 24h exposure to particles 4, 5 and 6 and measured by FCM. (*) shows the statistically significant difference (P<0.005). Data shows means ±SD

VII. Discussion

Nanomaterials such as graphene and its derivatives have been massively produced and attracted tremendous attention. Previous studies with different cellular or animal model have demonstrated that some of the graphene derivatives induced significant cytotoxicity and genotoxicity. It has been reported that the surface properties, shape, size, surface charge, stability and purity of the nanomaterials all contribute to the differential toxicity observed (Park et al., 2015; Wang et al., 2013). Also for graphene-based materials it was reported that the different physicochemical properties result in different cellular toxicities (Ou et al., 2017; Zhang et al., 2014).

In this work the cellular effects of well-characterized GFNs were investigated to address the influence of them in morphology and viability of RAW264.7 cells.

Cellular uptake of nanoparticles is an important process and activates further biological effects inside the cell. To quantitatively evaluate the cellular uptake of GNFs flow cytometry was used and related the increase in flow cytometric side scatter (SS) intensity with an increase in intracellular GFNs. Cellular uptake results showed an increased in SS in all three conditions tested: 4h incubation at 4ºC, 4h incubation at 37ºC and 24h incubation at 37ºC. In the first condition, RAW264.7 cells were exposed to the GFNs at 4º C during 4h, and both concentrations (0.5BMD30 and BMD30) in P2, P3, P5, and P6, and the concentration BMD30 in P1, P4 and P7 showed significant increase comparing with control. In the second condition, RAW264.7 cells were exposed to the GFNs at 37ºC during 4h and only P4 at 0.5BMD30 concentration didn't show significant increase comparing with control. In the third condition the RAW264.7 cells were expose to the GFNs at 37ºC during 24h and P1, P2, P3, P5, P6 and P7 in both concentrations, and the concentration BMD30 in P4 showed significant increase comparing with control. To evaluate the effect of incubation temperature and duration of exposure a *t*-test was perform. The results suggested that at 37ºC had more internalization of GFNs than 4ºC, as expected since at 4ºC the phagocytic activity is inhibited (Lee et al., 2017). The duration of the exposure also influenced the internalization at 37ºC, because after 24h of exposure to GFNs more particle internalization occurred

specially for P1, P2, P3, P5 and P6. By comparing all the nanomaterials, those internalized at higher ratios were P3, P4 and P5 (carboxyl graphene, graphene nanoplatelets and graphene oxide powder, respectively). The differential mechanism of toxicity of GFNs can depend on their cellular uptake, as was described by Chatterjee and co-workers (2014) when exposed HepG2 to GO and rGO. Their results showed that GO (hydrophilic) has been internalized by the HepG2 cells, but rGO (hydrophobic) was adsorbed and aggregated at cell surface without (or lower) uptake influencing their toxicity.

ROS can be generated either by direct pro-oxidant effect of the GFNs or endogenously upon interaction with cellular material. DCFH-DA probe was used to determine the generation of ROS in the presence of GFNs using FCM analysis. The internalization of the GFN's had demonstrated influence in ROS production and in different ways. The nanomaterials P2, P3, P4, P6, and P8 showed an increase of ROS production at low toxicity levels (0.5BMD30) and not at BMD30 concentrations.

Comparing P4 and P7, both graphene nanoplatelets (2-10nm thickness) and reference pristine graphene nanoplatelets respectively, the results showed for P4 a significant increase of ROS levels but not for P7. This difference may be explained by the highest nanomaterial internalization observed for P4.

Higher ROS production has been often highlighted as a major cause for GFNs toxicity in several cell types. Previous studies in TPH-1 cells after layered graphene nanoplatelets exposure demonstrated loss of membrane integrity that could be due to generation of ROS (Jastrzebska et al., 2012). Yan and co-workers (2017) found a significant increase of ROS production after the exposure of THP-1 cells to GO and rGO with greater expression in the latter. In RAW64.7 cells exposed to CNT, carbon-black and nano-graphite, Figarol and co-workers (2015) found increased ROS production in a dose-dependent manner. HepG2 cells upon exposure to GO and carboxyl graphene, showed dose and time-dependent cytotoxicity with plasma membrane damage and induction of ROS, but not at low concentrations (<4µg/ml) (Sing et al., 2016). A concentration-dependent ROS induction, after exposure to GO, was reported for human skin fibroblast (Jastrzebska et al., 2012)

Through the evaluation of cellular uptake and ROS generation this work demonstrated that GFNs produce cytotoxicity in dose- and time- dependent manners.

Considering the ranking of toxicity, based on the concentration of nanoparticles per area that generate toxicity, the cellular uptake and ROS production show that P4, P5 and P6 are more toxic being P7 and P8 the less toxic to RAW264.7 cells. Therefore, P4, P5, and P6 were selected for further studies on the induction of apoptosis and effects on mitochondrial membrane potential.

Apoptosis was assessed combining the probe Annexin V and PI and further evaluation by FCM analysis. The results showed that P4 and P5 increased the number of apoptotic cells. When the cells were exposed to P4 the results showed significant increase in late and early apoptosis and P5 in early apoptosis and necrosis, demonstrating that modulation of apoptosis exists when exposure to these nanomaterials. P6 didn't show significant differences between control and exposed cells after 24h. Since previously described graphene is manufactured from graphite, and between P5 and P6 we can see that the latter, graphite oxide powder, didn't produce toxicity contrarily to P5, graphene oxide powder (S method), demonstrating that the physico-chemical characteristics influence the toxicology. Ou and co-workers (2017) demonstrated that graphene layers (10µg/ml) exposed to PC12 cell line induced apoptosis by activation caspase-3 in a time-dependent manner.

The mitochondrial membrane potential was assessed combining the probe Rhodamine 123 and PI, and then analysed by FCM. This experiment showed significant decrease in the MMP of P4 at both concentrations and P5 at BMD30 concentration. P6 didn't show significant differences between control and exposed cells after 24h. Disruptions of the MMP may cause severe physiological consequences including decrease in ATP synthesis, increase in ROS generation, and the redistribution of pro-apoptotic mitochondrial factors.

Li and co-workers (2012) reported that when RAW264.7 cells were exposed to pristine graphene destroys the MMP and increases intracellular ROS to cause cytotoxicity and subsequently trigger apoptosis. Graphene also induces cytotoxic

effects and mitochondrial injury in human neuronal cells at dose of 10µg/ml (Jastrzebska et al., 2012).

VIII. Conclusions – Future Perspectives

This study demonstrated that the duration and time of exposure to the GFNs influence the internalization in RAW264.7 cells, and the exposure of GFNs influence the ROS production. The different levels of toxicity are widely dependent of their physico-chemical characteristic.

Considering that humans are usually exposed to GFNs, especially at their manufacture, it is important to determine if or which GFNs are more cytotoxic. This study suggests that from all the GFNs studied, P4 and P5 (graphene nanoplatelets and single-layer graphene oxide powder, respectively) were the most cytotoxic to RAW264.7 cells and was successfully established cytotoxicity ranking of GFNs.

For future studies the biological effects of GFNs, its genotoxic potential, can be assessed on different types of cells. Also, a deeper study on the mechanisms underlying cytotoxicity by GFNs could be performed, for instance, the analysis of cytochrome c to better understand the relation between mitochondrial physiology and the release of cytochrome in apoptosis initiation. ATP measurements, protein expression and autophagy studies are also recommended.

Considering the position of graphene and its derivatives in the nanotechnology field in the lastet years, it is important to keep further research with fundamental and experimental studies.

IX. References

Amin, M. T., Alazba, A. A., & Manzoor, U. (2014). A review of removal of pollutants from water/wastewater using different types of nanomaterials. *Advances in Materials Science and Engineering, 2014*.

Arora, S., Dev, K., Agarwal, B., Das, P., & Syed, M. A. (2017). Macrophages: Their role, activation and polarization in pulmonary diseases. *Immunobiology, 233 (2)*

ATCC. (2016). *RAW 264.7 (ATCC® TIB-71™)*. Obtained of ATCC: https://www.lgcstandards-atcc.org/products/all/TIB-71.aspx?geo_country=pt

Buzea, C., Pacheco, I. I., & Robbie, K. (2007). Nanomaterials and nanoparticles: Sources and toxicity. *Biointerphases*, *2*(4), MR17-MR71.

Bussy, C., Ali-Boucetta, H., & Kostarelos, K. (2012). Safety considerations for graphene: lessons learnt from carbon nanotubes. *Accounts of chemical research*, *46*(3), 692-701.

Chang, Y., Yang, S.-T., Liu, J.-H., Dong, E., Wang, Y., Cao, A., et al. (2011). In vitro toxicity evaluation of graphene oxide on A549 cells. *Toxicology Letters, 200 (3)*, 201-210.

Chatterjee, N., Eom, H. J., & Choi, J. (2014). A systems toxicology approach to the surface functionality control of graphene–cell interactions. *Biomaterials*, *35*(4), 1109-1127.

Feynman, R. P. (1960). There's plenty of room at the bottom. *Engineering and science*, *23*(5), 22-36.

Figarol, A., Pourchez, J., Boudard, D., Forest, V., Akono, C., Tulliani, et al. (2015). In vitro toxicity of carbon nanotubes, nano-graphite and carbon black, similar impacts of acid functionalization. *Toxicology in Vitro*, *30*(1), 476-485.

Geim, A. K. (2009). Graphene: status and prospects. *Science*, *324*(5934), 1530-1534.

Gerencser, A. A., Christos, C., Birket, M. J., Martin , J., Vitelli, C., Nicholls, D. G., & Brand, M. D. (2012). Quantitative measurement of mitochondrial membrane potential in cultured cells: calcium-induced de-and hyperpolarization of neuron mitochondria. *The Journal of Physiology – Neuroscience, 590 (12)*, 2845-2871.

Gottlieb, E., Armour, S., Harris, M., & Thompson, C. (2003). Mitochondrial membrane potential regulates matrix configuration and cytochrome c release during apoptosis. *Cell Death and Differentiation*, 709-717.

Hingorani, R., Deng, J., Elia, J., Mclntyre, C., & Mittar, D. (2011). Detection of Apoptosis Using the BD Annexin V FITC Assay on the BD FacsVerse tm System. *BD Biosciences*.

Hirsch, Andreas. 2010. “The Era of Carbon Allotropes.” *Nature Materials* 9 (11).

Huang, J., Zong, C., Shen, H., Liu, M., Chen, B., Ren, B., & Zhang, Z. (2012). Mechanism of Cellular Uptake of Graphene Oxide Studied by Surface-Enhanced Raman Spectroscopy. *Small*, *8*(16), 2577-2584.

Ibuki Y., Toyooka T. (2012) Nanoparticle Uptake Measured by Flow Cytometry. In: Reineke J. (eds) Nanotoxicity. Methods in Molecular Biology (Methods and Protocols), vol 926. Humana Press, Totowa, NJ

Jastrzębska, A. M., Kurtycz, P., & Olszyna, A. R. (2012). Recent advances in graphene family materials toxicity investigations. *Journal of Nanoparticle Research*, *14*(12), 1320.

Jiang, W., Kim, B. Y., Rutka, J. T., & Chan, W. C. (2008). Nanoparticle-mediated cellular response is size-dependent. *Nature nanotechnology*, *3*(3), 145-150.

Joshi, D. C., & Bakowska, J. C. (2011). Determination of Mitochondrial Membrane Potential and Reactive Oxygen Species in Live Rat Cortical Neurons. *Journal of Visualized Experiments*, 1-4.

Kou, L., Sun, J., Zhai, Y., & He, Z. (2013). The endocytosis and intracellular fate of nanomedicines: Implication for rational design. *Asian Journal of Pharmaceutical Sciences*, *8*(1), 1-10.

Kumar, A., Pandey, A. K., Singh, S. S., Shanker, R., & Dhawan, A. (2011). A Flow Cytometric Method to Asses Nanoparticle Uptake in Bacteria. *International Society for Advancement of Cytometry, 79 (9)*, 707-712.

Li, Y., Liu, Y., Fu, Y., Wei, T., Guyader, L. L., Gao, G., et al (2012). The triggering of apoptosis in macrophages by pristine graphene through the MAP and TGF-beta signaling pathways. *Biomaterials, 33 (2),* 402-411.

Lu, C.-J., Jiang, X.-F., Junaid, M., Ma, Y.-B., Jia, P.-P., Wang, H.-B., & Pei, D.-S. (2017). Graphene oxide nanosheets induce DNA damage and active the base excision repair (BER) signaling pathway both in vitro and in vivo. *Chemosphere 184*, 795-305.

Ly, J. D., Grubb, D. R., & Lawen, A. (2003). The mitochondrial membrane potential in apoptosis; an update. *Apoptosis*, *8 (2),* 115-128.

Ma-Hock, L., Strauss, V., Treumann, S., Küttler, K., Wohlleben, W., Hofmann, et al. (2013). Comparative inhalation toxicity of multi-wall carbon nanotubes, graphene, graphite nanoplatelets and low surface carbon black. *Particle and fibre toxicology*, *10*(1), 23.

Matesanz, M. C., Vila, M., Feito, M. J., Linares, J., Gonçalves, G., Vallet-Regi, et al. (2013). The effects of graphene oxide nanosheets localized on F-actin filaments on cell-cycle alterations. *Biomaterials*, *34*(5), 1562-1569.

Menezes, C., Mendes, A., Farcal L., Ziemann, C., et al. (2017). Cytotoxicity and genotoxicity of graphene-family nanomaterials in RAW 264.7 mouse macrophages *Toxicology Letters, 280S* (2017) S180–S190

Omlor, A. J., Nguyen, J., Bals, R., & Dinh, Q. T. (2015). Nanotechnology in respiratory medicine. *Respiratory research*, *16*(1), 64.

Ou, L., Lin, S., Song, B., Lai, R., & Shao, L. (2017). The mechanisms of graphene-based materials-induced programmed cell death: a review of apoptosis, autophagy, and programmed necrosis. *International Journal of Nanomedicine, 12*, 6633-6646.

Ou, L., Song, B., Liang, H., Liu, J., Feng, X., Deng, B., et al. (2016). Toxicity of graphene-family nanoparticles: a general review of the origins and mechanisms. *Particle and fibre toxicology*, *13*(1), 57.

Park, E. J., Lee, G. H., Han, B. S., Lee, B. S., Lee, S., Cho, M. H., et al. (2015). Toxic response of graphene nanoplatelets in vivo and in vitro. *Archives of toxicology*, *89*(9), 1557-1568.

Rastogi, S. K., Raghvan, G., Yang, G., & Cohen-Karni, T. (2017). Effect of Graphene on Nonneuronal and Neuronal Cell Viability and Stress. *NanoLetters*, *17 (5),* 3297-3301.

Sanchez, V. C., Jachak, A., Hurt, R. H., & Kane, A. B. (2012). Biological Interactions of Graphene-Family Nanomaterials - An Interdisciplinary Review. *Chem. Res. Toxicol.*, *25* (1) 15-34.

Sasidharan, A., Panchakarla, L. S., Sadanandan, A. R., Ashokan, A., Chandran, P., Girish, et al. (2012). Hemocompatibility and Macrophage Response of Pristine and Functionalized Graphene. *Small*, *23;8(8)*, 1251-1263.

Scaduto, R. C., Jr, & Grotyohann, L. W. (1999). Measurement of Mitochondrial Membrane Potencial Using Fluorescent Rhodamine Derivatives. *Biophysical Journal*, *76 (1),* 469-477.

Shen, H., Zhang, L., Liu, M., & Zhang, Z. (2012). Biomedical applications of graphene. *Theranostics*, *2* (3), 283.

Singh, V., Joung, D., Zhai, L., Das, S., Khondaker, S. I., & Seal, S. (2011). Graphene based materials: past, present and future. *Progress in materials science*, *56*(8), 1178-1271.

Sing, Z. (2016). Applications and toxicity of graphene family nanomaterials and their composites. *Nanotechnology, Science and Applications*, *9*, 15-28.

Stern, S. T., & McNeil, S. E. (2008). Nanotechnology safety concerns revisited. *Toxicological sciences*, *101*(1), 4-21.

Suzuki, I., Toyooka, T., & Ibuki, Y. (2007). Simple and Easy Method to Evaluate Uptake Potencial fo Nanoparticles in Mammalian Cells Using a Flow Cytometric Light Scatter Analysis. *Environmental Science & Technology*, *41* (8), 3018-3024.

Vermes, I., Haanen, C., & Reutelingsperger, C. (2000). Flow cytometry of apoptotic cell death. *Journal of Immunological Methods*, *243* (1-2) 167-190.

Wang, A., Pu, K., Dong, B., Liu, Y., Zhang, Z., Duan, W., & Zhu, Y. (2013). Role of surface charge and oxidative stress in cytotoxicity and genotoxicity of graphene oxide towards human lung fibroblast cells. *Journal of Applied Toxicology*, 1156-1164.

Yan, J., Chen, L., Huang, C. C., Lung, S. C. C., Yang, L., Wang, W. C., et al. (2017). Consecutive evaluation of graphene oxide and reduced graphene oxide nanoplatelets immunotoxicity on monocytes. *Colloids and Surfaces B: Biointerfaces*, *153*, 300-309.

Zhang, Q., Wu, Z., Li, N., Pu, Y., Wang, B., Zhang, T., & Tao, J. (2017). Advanced review of graphene-based nanomaterials in drug delivery systems: Synthesis, modification, toxicity and application. *Materials Science and Engineering: C 77* (1), 1363-1375

Zhang, Y., Dayton, P., Xu, Y., Mahmood, M., Karmakar, A., Casciano, D., et al. (2014). Toxicity and efficacy of carbon nanotubes and graphene: the utility of carbon-based nanoparticles in nanomedicine. *Drug Metabolism Reviews*, *46* (2), 232-246.

Zhou, H., Zhao, K., Li, W., Yang, N., Liu, Y., Chen, C., & Wei, T. (2012). The interactions between pristine graphene and macrophages and the production of cytokines/chemokines via TLR- and NF-kB-related signaling pathways. *Biomaterials*, *33* (29), 6933-6942.

Zhou, X., Dorn, M., Vogt, H., Spermann, D., Yu, W., Mao, Z., et al.(2014). A quantitive study of the intracellular concentration of graphene/noble metal nanoparticle composites and their cytotoxicity. *Nanoscale*, *6* (15) 8535-8542.